Wind Energy Potential at Elevated Hub Heights in the U.S. Midwest Region

Bin Cai[1], Phuong Vo[2], Sri Sritharan[3*], M. ASCE, and Eugene S. Takle[4]

[1] *Postdoc Research Associate, Department of Civil, Construction, and Environmental Engineering, Iowa State University, Ames, IA 50011, USA*

[2] *Structural Engineer, WHKS & Co., Springfield, IL 62703, USA*

[3] *Wilkinson Chair Professor, Department of Civil, Construction, and Environmental Engineering, Iowa State University, Ames, IA 50011, USA*

[4] *Distinguished Professor Emeritus, Department of Agronomy, Iowa State University, Ames, IA 50011, USA*

ABSTRACT

The U.S. Midwest successfully generates wind power at a hub height of 80 – 90 m and the use of tall towers can reduce the wind energy cost. However, lack of reliable wind data and production estimates at elevated heights hamper this effort. In this paper, wind resources and annual energy production (AEP) are studied using wind data up to 200 m above ground to estimate and validate AEP as a function of hub height at multiple sites. The AEP results show that energy production can increase by about 10% when the hub height is increased to 100 m. It also suggests that the optimal elevated hub height for a given region is not constant. A suitable site-specific height is desirable to minimize the levelized cost of energy (LCOE). Wind information from the National Renewable Energy Laboratory Wind Integration National Dataset (WIND) Toolkit is used as an alternative for estimating AEPs at elevated hub heights. This approach produced somewhat conservative results, confirming its use for wind farm planning purposes when measured wind data are not available.

KEYWORDS

tall tower; wind speed; annual energy production; levelized cost of energy; WIND Toolkit

*Correspondence

Sri Sritharan, Department of Civil, Construction, and Environmental Engineering, Iowa State University, 376 Town Engineering, 813 Bissell Road, Ames, IA 50011-1066, USA.
Email: sri@iastate.edu

INTRODUCTION

Wind power generation has been fast-growing, providing 7% of the total electricity supply in the U.S. in 2019 and has now become the top renewable energy source (American Wind Energy Association [AWEA] 2020). This increasing trend is expected to continue with technological advancements to the wind energy system's major components and gradually reduce the levelized cost of energy (LCOE). The LCOE of wind energy has decreased by nearly 40% within the past decade in the U.S. as the rotor size, tower height, and turbine capacity have increased (DOE 2015a, b). According to AWEA (2020), a marked increase of 44% has been observed in rotor size and turbine capacity over the past decade in the U.S. These increasing trends cannot be sustained unless there is a corresponding increase in the hub height. However, the tower height continued to remain constant at 80 m until 2016 and then gradually increased by 13% to 90 m (AWEA 2020). This slow improvement in tower height is a drawback as taller towers will facilitate wind energy capture in better-quality wind resources, thereby increasing the annual energy production (AEP) and potentially reducing the LCOE (Hirth and Müller 2016; Lantz et al. 2019; Wiser et al. forthcoming). Estimating AEP for tall towers cannot be easily accomplished for a site in the U.S. due to the lack of available estimates of wind resources at elevated hub heights. The required data may be obtained either by installing wind instruments to collect field data or by conducting numerical analysis to model the wind data variation with height based on historical information. A primary concern in collecting field data is that installation and maintenance of tall meteorological towers are costly and that the instruments need to be deployed on the site for at least one year.

Although the wind resource estimates are not widely available for actual wind project sites, wind energy prediction is an important component of the LCOE estimate and can vary substantially with height. Reliable estimates of increased AEP can be taken as indicatives of the benefit of developing tall tower technologies, which help realize the LCOE reduction and justify the use of tall towers. Although tall tower technologies have been introduced for the U.S. market, their costs have not been fully realized since they have not been widely deployed (e.g., Engström 2010; MidAmerican 2015; Sritharan 2016; Barutha et al. 2019), limiting the investigation on LCOE. Therefore, this paper focuses on estimating the AEPs at elevated hub heights using two different wind data sources and making appropriate recommendations. The wind data sources included in the study are the measured wind data and the simulated data published by the National Renewable Energy Laboratory (NREL) via Techno-Economic Wind Integration National Dataset (WIND) Toolkit (Draxl et al. 2015)—a commonly-used public online database. The measured wind data were obtained from five sites in Iowa and one site in Minnesota over heights up to 200 m elevations. For the simulated data, WIND Toolkit, which was established using Weather Research and Forecasting (WRF) model to simulate the wind resource information, is applied with appropriate local conditions for all Iowa sites.

This paper first examines the wind speed variation with height and assess how accurately power laws represent this variation. Next, the calculation procedure for estimating the AEP variations with height and time is presented. After that, the calculation procedure is validated and then applied to the datasets mentioned earlier for all chosen sites to estimate the energy productions at elevated heights. Finally, by discussing the AEP and capacity factor trends with height, the paper concludes with appropriate recommendations in the context of using tall towers in wind energy production.

SUMMARY OF PREVIOUS STUDIES

Several studies have explored the correlation between wind speed and height, leading to the power-law relationship between the two variables (Davenport 1961). Historically, a power-law exponent of 1/7 has been used when a more refined value based on wind data is not available (Hennessey 1977; Storm 2009; Walton et al. 2014). This relationship was investigated by Takle et al. (1978) using a 32-m instrumented tower in Iowa, which confirmed the appropriateness of the 1/7 power-law exponent. However, more recent studies that utilized in-situ measurements indicated that the constant power-law would not adequately characterize the wind speeds at higher altitudes that are suitable for the operation of wind turbines supported by tall towers. By examining the wind data between 100 m and 150 m heights from six locations for the duration of July 2006 to March 2007, Redburn (2007) showed substantial diurnal and seasonal variations of wind speed with height in Missouri. It was also found that the increase in wind speed, as the height increased, was the greatest during nighttime hours in winter and early spring while it was the least during daytime hours in fall and late spring. This trend was further confirmed with a longer period of observations at more locations in the Midwestern states (Schwartz and Elliott 2005; Walton et al. 2014). These studies also concluded that 1/7 power-law exponent might not be appropriate for establishing wind speeds at elevated heights as it is influenced by the seasonal and diurnal variations and that more suitable exponent values should be established using wind speeds obtained at higher elevations. Additional analysis of wind characteristics within the rotor layer for tall wind turbines (i.e., between 50 and 200 m) revealed that power-law exponents generally exceed the 1/7 value (Kelley et al. 2004;

Petersen et al. 1998). The higher values regularly occur in winter during nighttime hours when wind speed is higher. This increased exponent and the corresponding wind speed are suggested to be carefully accounted for in predicting the AEP.

There have also been several attempts to model wind resources and estimate AEPs at higher heights by using some form of statistical reanalyses or numerical forecasting models. Using statistical models and historical wind farm data such as wind speed and power output, and in some cases including wind direction and atmospheric parameters, statistical reanalyses have proven to be an effective approach to determine the wind speed at different heights (Gualtieri and Secci 2012) and predict the wind power potential (Duran et al. 2007; Frank et al. 2020). Although the results from these studies showed good agreement with the short-term measured wind data (i.e., several hours and days) at high elevations, only limited validation is available using long-term wind measurements. Apart from the statistical models, the WRF model has been commonly adopted for numerical simulations to predict wind resources and power production at elevated heights. Storm et al. (2009) evaluated the WRF model using different configurations in forecasting wind shear for specific regions in Texas and Kansas. When compared with the field observations, these results were found to underestimate the wind speeds, although they were more accurate than the results from using the constant 1/7 power law. Draxl et al. (2015) developed a wind data repository using the WRF model and previous wind data recordings. Since this data repository includes all states in the U.S., limited validation opportunities are available to verify the modeling output for all the locations.

Furthermore, among the different modeling approaches used for wind power prediction, few have used site-specific data to model the wind resource (Duran et al. 2007; Frank et al. 2020; Storm et al. 2009), and thus the reliability of the modeling methods was not justified. By analyzing the local wind resource reflecting the site-specific geography and wind conditions at elevated heights, studies (Burt 2017; Johansson and Thorson 2016) have shown that including wind data at the micro-scale improves the accuracy of wind energy prediction. Their results also suggests that the availability of site-specific data at the micro-scale was a crucial component in determining whether it is feasible and economically beneficial to develop tall wind projects for a given site.

WIND DATA

As noted, this study utilizes two different data sets: measured wind data and simulated data from WIND Toolkit. Measured wind data used in this study are summarized in Table 1, including the locations of various stations. The field data in Iowa were acquired from the Iowa Energy Center and measured from wind meteorological towers at five wind stations, namely Quimby, Palmer, Mason City, Altoona, and Homestead (AWS Truepower 2010), as identified in Fig. 1. These sites are located in different wind resource regions, as shown in Fig. 1, which also depicts the wind speed at 80 m elevation. The northwestern sites have relatively more favorable wind conditions than those in the southeastern part of the state. These five towers were instrumented at 50, 100, 150, and 200 m to collect wind-energy resource data from December 2006 to April 2009, except Palmer, which was not instrumented at 200 m. The acquired wind data characteristics included temperature, mean wind speed, wind speed standard deviation, mean wind direction, and wind direction standard deviation. All measurements were recorded at 10-minute intervals for all heights, and the time was recorded in local standard time.

The data at meteorological towers, including periods of downtime when icing and lightning events occurred, were collected by sensors and controlled by replacing missing times with “NaN”. For a detailed description of the datasets used in Iowa, the reader can refer to the study completed by Walton et al. (2014). To demonstrate the analyses of the wind data and estimation of AEPs at different heights, Homestead is used herein as an example site. Missing or unavailable data for Homestead, IA from heights 50 to 200 m are indicated in Table 2.

The wind speed and direction data were chosen to characterize the diurnal and seasonal variations of wind shear in the rotor layer, which is between 50 and 150 m. Within this range, wind measurement data loss was less than 5%; data loss of above 30% occurred to the wind direction measurement at 100 m in Homestead, IA. In addition, wind speed data were validated as part of this study by comparing against the measurements from nearby wind stations to ensure that the collected data sufficiently represent the wind speed variations over time. Note that the wind speed data losses at this site for heights from 50 to 150 m are small, which also applies to the remaining sites. Since these values are small and AEP is calculated based on the accumulation of average hourly energy productions in this study, it is acceptable to exclude the missing wind speeds from this range when determining the wind characteristics and energy productions at the desired hub height.

To calculate AEP, two methods were tested. It was found that the AEP values at the height of 100 m were comparable to those averaged from the AEP estimates based on the wind data at 50 and 150 m. Similarly, hub-height AEPs at the Minnesota site, which will be introduced in the following data description, were found to be within negligible differences with those averaged from the AEP estimates at the top and bottom of the rotor layer. For this reason, analyses are completed using the wind speed at the hub height to predict the wind energy potential of tall towers as it requires fewer data and computations. Regarding the information used to assess the energy production for hub heights up to 140 m, only wind speed distribution from 50 to 150 m is needed as this range covers the hub height in which rotors are operating.

The field dataset required for the Minnesota site was obtained from the Eolos wind research station at Rosemount, MN, which provides wind measurements including wind speed, wind direction, temperature, air density and pressure, and humidity (Showers 2014). This monitoring center records information from a Clipper Liberty 2.5 MW wind turbine and a 130 m (426 ft.) tall meteorological tower, which was instrumented at ten different heights to record wind data every one minute. As with the Iowa data, each dataset from Rosemount was filtered by replacing unavailable and error data points with "NaN"s to eliminate the effects of random events.

As previously noted, data used for analyzing energy production also include numerically simulated datasets from the NREL Techno-Economic WIND Toolkit. The corresponding wind data include information such as wind speed and direction, temperature, air density, and pressure of more than 126,000 wind farm sites across the nation at a five-minute interval from January 2007 to December 2012 (Draxl et al. 2015; King et al. 2014). Again, Homestead is used as an example site to examine the simulated data based on the WIND Toolkit and to determine how well this data could be used to estimate AEP. Energy productions are then summarized for other sites in IA based on the simulated data and compared with those estimated from actual measurements, validating the potential to use WIND Toolkit data in estimating wind energy when measured wind data are not available.

METHODOLOGY

Prediction of the energy production potential from a wind turbine or a wind plant depends on estimates of wind speeds within the rotor layer and turbine capacity. Since the wind speeds increase nonlinearly with height, the power-law relationship is used to calculate wind speeds for desired heights using the following equation: (Davenport 1961)

$$\frac{u_2}{u_1} = \left(\frac{z_2}{z_1}\right)^{\alpha} \tag{1}$$

where u_1 and u_2 are the wind speeds measured at heights $z_1$and z_2, respectively. Note that the wind speed observations u_1 and u_2 are in the form of either time histories or average values for a specified period (e.g., 10-minute intervals). The power-law exponent α, which falls in the range of $0.05 \leq \alpha \leq 0.5$, has been frequently taken as 1/7 when adequate topographic information is unavailable (Takle et al. 1978). This constant value has been used for estimating wind power productions (Moné et al. 2015).

To capture the variations of wind speed v_i calculated from Eq. (1) over the chosen time interval, Weibull distribution, as commonly adopted, is used to characterize the frequency distribution of wind speed (Celik 2004; Bustamante et al. 2008; Deaves and Lines 1997; Hennessey 1977). This approach is preferred because it simplifies the AEP calculation; the use of the entire data set directly in the AEP calculations is unnecessarily cumbersome. The probability density function for Weibull distribution is defined using Eq. (2)

$$f(v_i; \eta, \beta) = \frac{\beta}{\eta}\left(\frac{v_i}{\eta}\right)^{\beta-1} exp\left[-\left(\frac{v_i}{\eta}\right)^{\beta-1}\right], v_i > 0 \tag{2}$$

where η is the shape factor depending on the flatness of the distribution, and β is the scale factor of the distribution. Both of these variables can be determined by statistical methods (Meeker and Escobar 1998). Incorporating the probability distribution of wind speeds with the provided power curve, annual energy production can estimate wind power potential on an annual basis and be calculated as shown in Eq. (3) to Eq. (5).

$$AEP_{gross} = \sum_{j=1}^{days}\left[\sum_{h=1}^{24}\left(\frac{\sum_{i=1}^{m} E(v_i)}{m}\right) \times 6\right] \tag{3}$$

$$E(v_i) = P(v_i)p(v_i) \tag{4}$$

$$AEP_{net} = AEP_{gross} \times losses \times availability \tag{5}$$

where v_i in this study uses 10-minute average wind speed established from the raw data unless otherwise noted, $P(v_i)$ is the power output, $p(v_i)$ is the number of occurrences for wind speed v_i obtained from fitting the Weibull distribution in Eq (2), and m is the total number of available data points for each hour per month, which accounts for any missing data. The product of power output and the number of occurrences for wind speed v_i provides wind energy production $E(v_i)$ for each wind speed increment. Summing the average hourly energy production $\frac{\sum_{i=1}^{m} E(v_i)}{m}$ for total hours within a single year provides the AEP. This approach for estimating the wind power potential is based on the use of the 10-minute frequency distribution of wind speed within each hour and the given power curve obtained from the turbine manufacturer. To determine AEP from a set of 1-minute average wind data acquired from Rosemount, the hourly power potential is computed by multiplying the 1-minute average energy production for each hour per month by sixty, the number of minutes in each hour. To verify that the 1-min wind data from Rosemount provide acceptable time-intervals, 10-min average wind data were tested and found that there were minimal differences in energy production at given heights. Therefore, this paper uses the original 1-min wind data for this particular site as this provides a means to examine the AEP production using different time intervals.

In this study, the net AEP is explicitly calculated for two utility-scale turbines, which are a 2.3 MW turbine with 108-m rotor diameter and a 3.2 MW turbine with 113-m rotor diameter. They were chosen since the power curves for these two Siemens turbines are readily available (Studylib 2017; Bauer and Matysik 2017).

According to the 2013 NREL Cost of Wind Energy Review (2015), the design life of turbines is assumed to be 20 years when estimating the economic outcomes from the AEP increase. In the AEP estimation, production losses, turbine availability, and atmosphere parameters (i.e., air density and altitude) are assumed to be constant as defined in the NREL report when the related information is not available. However, for Rosemount, air density is adjusted by converting the ambient temperature to virtual temperature for different hub heights (List 1951). Monthly energy production from the varied air density shows less than a 2% difference compared to the results from the non-adjusted air density, justifying the use of a constant air density for the Iowa sites.

The other significant quantity to evaluate wind energy production is the capacity factor, which can be obtained from the net AEP and calculated from Eq. (6).

$$Net\ capacity\ factor = \frac{AEP_{net}}{turbine\ capacity \times 8760} \times 100\% \tag{6}$$

where turbine capacity is the nominal power capacity for a selected turbine and AEP_{net} is the net annual energy production determined from Eq. (5). Since all calculations in this paper include the assumed losses and reduction factors, reported AEP and capacity factor in the remainder of the paper reflect the net production.

WIND CHARACTERISTICS

The measured wind data at 100m from Homestead is used to assess the ability of the AEP model to estimate wind energy production. To execute the same, wind speed and power-law exponent are first analyzed using the relationship outlined in Eq. (1). Hourly averages of wind speeds obtained from the on-site measurements at 100 m are plotted as a function of time in Fig. 2. This figure exhibits different diurnal trends of wind speed for the four meteorological seasons. Field measurements show higher wind speeds during nighttime (1800 – 0600 LST, where LST stands for Local Standard Time) than daytime (0600 – 1800 LST), which agrees well with the diurnal patterns of wind speeds from early studies (Walton et al. 2014; Kelley et al. 2004). Wind speeds from the field samples show their maximum near midnight and decrease to their lowest at approximately mid-morning. The mean wind speed at nighttime is between 6.0 and 8.0 m/s in the summer (June, July, August, i.e., JJA) and between 8.5 and 9.5 m/s during the following seasons: spring (March, April, May, i.e., MAM), fall (September, October, November, i.e., SON), and winter (December, January, February, i.e., DJF). During the daytime hours, the mean wind speed differs less than that observed for the nighttime hours and shows an average of 5.5 m/s in the summer and 7.9 m/s in other seasons. Although the wind speeds during the summer are lower than other seasons, the diurnal variations exhibit a similar pattern to the other seasons.

The power-law exponent is determined for using wind speeds at 50 m and 150 m based on Eq (1) and is plotted in Fig. 3 (Walton et al. 2014). Compared to the actual power-law exponents, it is clear that the commonly used theoretical value of 1/7 does not adequately represent the diurnal variation occurring between 50 m and 150 m, which is the rotor layer for utility-scale wind turbines. The International Electrotechnical Commission (IEC) Standard, labeled as a dotted line, suggests a higher value of 0.2 to represent the Normal Wind Profile (NWP) in Iowa, but it also fails to capture the actual distribution of the power-law exponent. Fig. 3(b) reflects the log-scale of the probability of the variation in the power-law exponent, which illustrates that using a single distribution function may not accurately fit the data (Smith et al. 2002). From the diurnal cycle plot in Fig. 3(a), it is further seen that using a constant value significantly underestimates the power-law exponent at nighttime when the production is expected to be high and slightly overestimates it during the daytime. The measured power-law exponent is in the range of 0.06 and

0.38, depending on the season and the hour. During the warm season (MAM, JJA), the variations of the power-law exponent are generally comparable to the cold season (DJF, SON), while the observed yearly nighttime exponents are generally three times higher than the daytime exponents. A power-law exponent higher than 0.2 during the nighttime implies a higher wind shear condition, which should be considered to minimize any operational challenges associated with wind turbines (Kelley et al. 2004). Since nighttime hours have higher wind speeds and higher power-law exponents than during the day, calculating the wind power production over 10 minutes is used to obtain accurate estimates of AEP.

VALIDATION OF AEP ESTIMATES

A comparison of the seasonal energy production is made between the calculated energy production and the hourly wind generation data recorded from Midcontinent Independent System Operator (MISO 2014). The historical wind generation data were reported every hour in a year at the MISO level. The probability of wind speed at 100 m is first found by fitting the one-year measured data to Weibull distribution using Eq. (2). The corresponding energy production is then calculated based on Eqs. (3-5). Data received from MISO are finally processed similarly to provide an average energy production for wind generation in the entire MISO Midwest region, in which varying hub height of 55 to 100 m is used. To minimize the effect of varying hub height, the average hourly energy production is normalized by dividing it by the total energy production and the result is presented in Fig. 4(a). Additionally included in this figure is the normalized energy production (labeled as MET) that is obtained from measured data in Homestead. The normalized energy production from Homestead shows more fluctuations than the MISO results, which exhibit much flatter diurnal patterns. This difference in the normalized production is not unexpected, primarily because the MISO data is likely to have been influenced by geographic smoothing. Additional reasons that can contribute to the difference between the calculated results and MISO data include the following: 1) the MISO energy production from wind is influenced by the market demand and unexpected turbine curtailment in individual wind farms, and 2) terrain condition and the hub height are variables in the MISO data. To improve the comparison with the MISO data, the normalized energy production for the measured data is averaged hourly over the entire observation period and reported as MET_ave at 4.1% in the figure. As can be seen, both averages compare closely, providing confirmation for the approach used for calculating AEP in this study.

The two data sources are further analyzed for their normalized seasonal productions, as presented in Fig. 4(b). Results for both MET and MISO normalized production demonstrate higher values during winter (DJF) and spring (MAM), whereas lower normalized production for summer (JJA) and fall (SON) seasons. A strong agreement in seasonal patterns between MET and MISO suggests that the AEP equation is a satisfactory model in providing annual energy production. The application of the AEP model has been adequate in not only calculating energy production but also representing seasonal variability, therefore making it a valuable tool for assessing case studies concerning other sites.

RESULTS

Energy production assessment

In Fig. 5, the calculated α for all six sites during the summer months, as expected, varies drastically from the commonly-assumed constant values. For the sites in IA, the variation of power-law exponent with time is examined by using wind speed data from all three summer months over the height from 50 m to 150 m, whereas the MN data reflect the average α established for July using wind data over a 30 m – 130 m height range due to limited data availability.

As seen in Fig. 5, all sites exhibit comparable diurnal patterns for α. For IA sites, some variations in power-law exponent are seen, especially at night, while the MN site shows consistently higher power laws compared to IA sites. For all sites, the minimum power-law exponents are obtained during the daytime (i.e., 0600-1800 LST) with the peak near midnight or early morning hours. The observed trends of the diurnal patterns are found to support historical measurements reported for the Midwest (Walton et al. 2014; Kelley et al. 2004; Smith et al. 2002). The exponent values for all the curves range from 0.26 to 0.46 at night while they vary from 0.01 to 0.09 during the day. Data from these sites also demonstrate that the hourly average exponents are estimated at 0.248 for the data duration and consistently deviate from constant values of 1/7 and 0.2, as previously noted. To accurately estimate the AEP for all of these sites, the respective power-law exponents shown in Fig. 5 are updated using the entire data for each site and then used in the power estimation. Wind speeds are computed for desired hub heights, namely 50 m, 80 m, 100 m, 120 m, and 140 m, using the respective power-law exponent for each site. Fig. 6 demonstrates the variations in average hourly wind speeds calculated for all available durations at different hub heights (see Table 1 for durations). As expected, wind speed increases with height at all sites and the vertical gradient of wind speed becomes more pronounced as the hub height increases. A persistent diurnal variation is seen for wind speeds above 80 m at all locations, showing higher values at night than during the day. However, at the relatively low elevation of 50 m, the highest wind speeds are observed during the mid-afternoon. As the sun rises during the day, the air near the surface ground becomes warmer and couples with the cooling air from the upper level, causing an opposite trend for the wind speed. The inversed diurnal variation at relatively low altitudes agrees with the historical wind speed trends in the Midwest (Takle et al. 1978; Storm et al. 2009; Walton et al. 2014; Kelley et al. 2004). Consistent with the lower power-law seen before, the variation in wind speed at different hub heights is insignificant during daytime (i.e., 0600-1800 LST). At Rosemount, the change in wind speed has a different trend and the corresponding magnitudes are slightly lower than the IA sites; this is partly due to using data from one summer month for this site.

Using the probability of wind speeds obtained from Weibull distribution and the corresponding power output from the appropriate power curves, the average annual energy productions are estimated based on Eqs. (2-5) for each site over the entire measurement period. Both the AEP and capacity factor are calculated in each case. Figs. 7 and 8 present the capacity factor for each IA site as a function of hub height, while Table 3 presents the average values for AEP and capacity factor obtained for all five sites. On average, raising hub height from 80 to 100 m increases the AEP by approximately 10% (Figs. 7, 8, and Table 3). New turbines in the U.S. typically have a hub height near 90 m. A similar increase is seen when the hub height increases from 100 m to 140 m, implying that the benefit in hub height increase is more significant for the first 20 m. This observation is confirmed in Figs. 7 and 8, which shows that the capacity factor can be increased by as much as 25% compared to 80 m tall towers by simply elevating the hub height to 140 m. It is also seen that the benefit of tall towers varies depending on the location, and therefore collecting wind data at the actual wind farm location is critical for realizing the optimal hub height for tall towers.

As the hub height increases, the capacity factors for both turbines increase significantly, reaching net capacity factors in the range of 48% to 52%. Although the production of a 3.2 MW turbine is higher than the 2.3 MW turbine due to its bigger turbine size and larger rotor diameter, the 2.3 MW turbine consistently produces higher capacity factors. This higher capacity factor is due to the specific power of the 2.3 MW being lower than that of the 3.2 MW turbine. However, when the benefits of the two turbine sizes are compared with respect to the tower height, Table 3 shows that the percentage increase in capacity factor is moderately higher for 3.2 MW with taller towers. The combination of higher AEP and percentage increase in capacity factor will favor the large-size turbine with an appropriate power curve for tall tower applications. By utilizing a bigger rotor to reduce the specific power, increases in capacity factor can also be realized for the 3.2 MW turbine. Figs 7(b) and 8(b) also show the capacity factor percentages, showing the relative differences in capacity factor at elevated heights respective to 80 m. It is observed that the percentage in capacity factor varies among the site, with all five sites presenting a capacity factor of above 42% for both turbines at 140 m. This observation again emphasizes that finding an optimal tower height using measured wind data for each localized region is important to fully realize the benefits of tall towers and minimize the LCOE. Moreover, it is clear that the lowest capacity factors for the two turbine configurations are between 33% and 37% at 80 m, which are higher than the average of 30.8% among all project samples built from 2004 to 2011 obtained for a recent wind market study published by the U.S. DOE (Wiser et al. 2019). This improvement is impacted by the industry trend of higher hub heights and lower specific power. Particularly, 20 m taller than the conventional hub height of 80 m already contributes to a 9% increase in capacity factor for all sites, which provides significant growth in wind resources.

Since the recorded period for Rosemount is short, the relationship between the capacity factor and hub height for this site is plotted separately in Fig. 9 for the 2.3 MW and 2.5 MW turbines. Compared to the average summer (JJA) values of the capacity factor in Iowa, Rosemount shows a similar upward increasing trend with hub height and the capacity factors in July are within 10% difference from the Iowa average values for a 2.3 MW turbine. The capacity factors for a 2.5 MW turbine are lower than the values for the 2.3 MW turbine, which is driven by the increase in turbine specific power, suggesting that estimating the wind energy production for elevated hub heights is greatly helpful for turbine and tower height selection.

Case study using WIND Toolkit data

Since measured wind data are not readily available for broader regions at elevated heights, this section examines the possibility of using the WIND Toolkit to estimate the wind speeds and evaluate the AEP at higher hub heights (Draxl et al. 2015). The Techno-Economic WIND Toolkit provides data for the entire U.S. at 120,000 locations. This WIND Toolkit contains 7-year data at a 5-minute interval at 100-m elevations. To examine the quality of the data, diurnal and seasonal variations for wind speeds at Homestead are first examined and compared to those obtained from measured wind data. The WIND Toolkit site chosen for this comparison is located within 2 miles of the Homestead site. As shown in Fig. 10(a), similar to the wind measurements obtained from the meteorological tower at 100 m, the maximum wind speed from the WIND Toolkit occurs at night and the minimum wind speed is experienced after sunrise. Additionally, the diurnal and seasonal variations obtained from the simulated wind data show similar trends to those obtained from the wind measurements. However, the seasonal averages of daytime (DT [0600 – 1800 LST]) and nighttime (NT [1800 –0600 LST]) wind speeds from the WIND Toolkit slightly underestimate the actual average values (Fig. 10(b)). This observation suggests that calculating the energy production using the WIND Toolkit would yield conservative results, but the difference between the Toolkit data and tower measurements would be minimal for the energy production estimates.

Next, the daytime (DT [0600 – 1800 LST]) and nighttime (NT [1800 –0600 LST]) wind roses at a 100 m height in Homestead are analyzed for each wind data source and their respective seasons, as displayed in Fig. 11. The seasonal and diurnal patterns from the measured data agree well with earlier findings that confirm wind speeds during daytime are likely to be lower than the nighttime values for all seasons and the maximum wind speed usually occurs during nighttime hours (Walton et al. 2014; Kelley et al. 2004). The WIND Toolkit results show a good agreement with tower measurements for all seasons but exhibit lower speed for northwest winds during the daytime and nighttime hours in winter, as shown in Fig. 10 and Fig. 11.

To examine the reliability of using the Toolkit in estimating AEP, Homestead is chosen as an example site to compares the daytime (DT) and nighttime (NT) energy production between the measured data and WIND Toolkit data. Using the actual power-law exponent calculated from wind speeds at 50 m and 150 m and the constant value of 1/7, Fig. 12 shows the calculated results for DT and NT energy productions. For the Siemens 2.3 MW turbine model, the increments in two types of energy productions that use measured power-law show similar trends for both the field and simulated data, while the energy productions calculated from the constant power law show a slower increase with the hub height during the day. This difference is impacted by diurnal variations of the power-law exponent captured in Fig 3. With this analysis, using daytime wind data from WIND Toolkit will underestimate the annual energy production. This inadequate estimate can be influenced by the low wind speeds modeled by the WIND Toolkit, as was discussed at the beginning of this section. Similar conclusions can also be made for the Siemens 3.2 MW turbine model. The total annual energy production calculated directly from the measured and WIND Toolkit data at 100 m are summarized in Table 4. Generally, WIND Toolkit underestimates the AEP by about 7.5% compared to the estimates obtained from the measured data.

Fig. 13 summarizes the average capacity factor obtained from all five sites in IA. This figure includes the 1/7 power law as a reference for comparing the effect of the measured wind shear. In general, using the Toolkit data would lead to some underestimation of the AEP at relatively lower hub heights while overestimating the values at heights above 120 m. Specifically, when the realistic wind shear is applied to the Toolkit data, the most considerable difference of the average capacity factor between the two data sources occurs at 80 m, for which the average capacity factor from Toolkit is 4.6% lower than the results obtained from the measured data. When compared at higher heights, Toolkit produces the largest overestimation at 140 m by 2.9% compared to that obtained from the measured wind data. Improvement of using the actual wind shear in AEP prediction is realized by comparing the largest difference of the average capacity factor at heights above 80 m to that calculated only with the constant wind shear. When only using the 1/7 power law, the Toolkit data consistently provides lower capacity factor predictions relative to the measured results. The most considerable difference between the two data sources occurs at 140 m and increases to 4.3%.

CONCLUSIONS

An analytical study was performed to investigate the wind energy potential of tall towers in the U.S. Midwest region (i.e., Iowa and Minnesota) using two different wind data sources: measurements taken from the specific sites and modeled data from the Techno-Economic WIND Toolkit. Wind speed and power-law relationship were first examined for the measured data at Homestead, IA. The corresponding AEP estimates were then validated by comparing the normalized energy production calculated from the estimated model with the reported wind generation data from MISO. Next, using the validated model and two different turbine configurations, AEPs and capacity factors were estimated for different desired hub heights using measured wind data at the six sites in the region. A similar effort was also undertaken to evaluate the wind potential at each site using the WIND Toolkit data in conjunction with the measured and theoretical power-law exponents. Based on the findings from this study, the following conclusions have been drawn:

- A similar diurnal variation of wind speed was seen consistently at the chosen sites for different seasons and tower heights, showing consistently higher wind speeds at night than during the day. With increased hub heights, nighttime wind speeds increased significantly, while a minimal change in wind speed was found during the day.
- In contrast to the theoretical constant value, wind data in Iowa and Minnesota sites featured significant variations of the power-law exponent as a function of time. These values were averaged to about 1/4 as opposed to a routinely-used value of 1/7 assumption. To obtain realistic AEP estimates, it is important to incorporate a power-law exponent as a function of time in the calculation.
- The AEP estimates were validated using measured wind data and varied power-law exponents. The calculation model for AEP estimates produced satisfactory results of energy production for a day and four seasons when compared to MISO records. Although MISO records presented more stable diurnal cycles of energy production than the measured data, the difference of annual averages between the two sources was minimal, indicating that the AEP calculation adopted in this study was suitable for assessing wind energy production.
- The energy production potentials generally showed an increase of more than 9% in AEP and capacity factor with a 20-m increase from a hub height of 80 m, indicating an advantage in raising the turbine height by at least 20 m in the wind-rich regions. While a further increase in

hub height was shown to be advantageous, it is important to use a site-specific optimal hub height for designing wind farms with tall towers as it would produce the lowest LCOE.

- Simulated data from WIND Toolkit were also used to estimate AEP and capacity factors for areas where limited or no field measurements were available. Wind data from the Toolkit were first examined for accuracy with the actual measurements and showed a good representation of the variation of the actual wind speed and direction at 100 m with lower estimates in wind speed, indicating a lower estimate for energy production.
- A less than 8% difference in energy production estimate was reflected for Homestead between the simulated data from the WIND Toolkit and the field measurements when the actual power-law exponent was used. However, the percentage increased up to 12% for 140-m wind towers if the constant value of the power-law exponent was used in the estimate, indicating that obtaining the power-law exponent from the actual wind project site or nearby available locations is critical to predicting wind power potentials at elevated heights.
- The WIND Toolkit may be used for estimating AEPs for tall towers. When realistic wind shear information was used, it was found that WIND Toolkit overestimated the AEP prediction by 2.9% at 140 m while underestimating the corresponding value by 4.3% when the wind shear was approximated to 1/7.

DATA AVAILABILITY STATEMENT

The wind resource data to validate the AEP increases and the files revealing the findings of this study are available upon reasonable request from the corresponding author.

ACKNOWLEDGMENTS

This study was partially funded by the Office of Energy Efficiency and Renewable Energy of the U.S. Department of Energy under Award No. DE-EE0006737. The authors are very grateful to the Iowa Energy Center for providing the wind resource data in Iowa and Eolos Wind Research Station at the University of Minnesota for providing additional wind data measurements.

REFERENCES

AWEA (American Wind Energy Association). 2020. "Wind Powers America Annual Report 2019." Washington, DC: AWEA.

AWS Truepower, Inc. 2010. *Final Report: Iowa Tall Tower Wind Assessment Project - Iowa State University.* Ames, IA: Iowa Energy Center.

Barutha, P., A. Nahvi, B. Cai, H. D. Jeong, and S. Sritharan. 2019. "Evaluating Commercial Feasibility of A New Tall Wind Tower Design Concept Using A Stochastic Levelized Cost of Energy Model." *Journal of Cleaner Production*, 240 (Dec): 118001. https://doi.org/10.1016/j.jclepro.2019.118001.

Bauer, L., S. Matysik. 2017. "Siemens SWT-3.2-113 Power Curve." Wind-turbine-model.com. Accessed July 18, 2017. https://en.wind-turbine-models.com/turbines/966-siemens-swt-3.2-113#datasheet.

Burt, M., J. Firestone, J. A. Madsen, D. E. Veron, and R. Bowers. 2017. "Tall Towers, Long Blades and Manifest Destiny: The Migration of Land-Based Wind from the Great Plains to the Thirteen Colonies." *Applied Energy,* 206 (Nov): 487–497. https://doi.org/10.1016/j.apenergy.2017.08.178.

Celik, A. N. 2004. "A Statistical Analysis of Wind Power Density Based on the Weibull and Rayleigh Models at the Southern Region of Turkey." *Renew Energy*, 29 (4): 593–604. https://doi.org/10.1016/ j.renene.2003.07.002.

Davenport, A.G. 1961. "The Spectrum of Horizontal Gustiness Near the Ground in High Winds." *Q J R Meteorol Soc*, 87 (372): 194–211. https://doi.org/10.1002/qj.49708737208.

Deaves, D. M., and I. G. Lines. 1997. "On the Fitting of Low Mean Windspeed Data to the Weibull Distribution." *J. Wind Eng Ind Aerodyn,* 66 (3): 169–178. https://doi.org/10.1016/S0167-6105(97) 00013-5.

DOE. 2010. "Iowa 80-Meter Wind Resource Map." Accessed June 21, 2017. https://windexchange.energy.gov/maps-data/32.

DOE. 2015a. "Enabling Wind Power Nationwide." Washington, DC: DOE.

DOE. 2015b. "Wind Vision: A New Era for Wind Power in the United States." DOE/GO-102015-4557. Washington, DC: DOE.

Draxl, C., A. Clifton, B. M. Hodge, and J. McCaa. 2015. "The Wind Integration National Dataset (WIND) Toolkit." *Appl. Energy,*151 (Aug): 355–366. doi:10.1016/j.apenergy.2015.03.121.

Duran, M. J., D. Cros, and J. Riquelme. 2007. "Short-Term Wind Power Forecast Based on ARX Models." *J. of Energy Eng.*, 133 (3): 172-180.

Engström, S., T. Lyrner, M. Hassanzadeh, T. Stalin, and J. Johansson. 2010. "Tall Towers for Large Wind Turbines Tall Towers for Large Wind Turbines Report from Vindforsk Project V-342 Höga Torn för Vindkraftverk Elforsk Rapport." 10:48. Stockholm, Sweden: Elforsk AB.

Frank, C. W., B. Pospichal, S. Wahl, J. D. Keller, A. Hense, and S. Crewell. 2020. "The Added Value of High Resolution Regional Reanalyses for Wind Power Applications." *Renewable Energy*, 148 (Apr): 1094-1109.

García-Bustamante, E., J. F. González-Rouco, P. A. Jiménez, J. Navarro, and J. P. Montávez. 2008. "The Influence of the Weibull Assumption in Monthly Wind Energy Estimation." *Wind Energy*, 11 (5): 483–502. https://doi.org/10.1002/we.270.

Gualtieri, G., and S. Secci. 2012. "Methods to extrapolate wind resource to the turbine hub height based on power law: A 1-h wind speed vs. Weibull distribution extrapolation comparison." *Renewable Energy*, 43 (Jul): 183-200. https://doi.org/10.1016/j.renene.2011.12.022.

Hennessey J. P. Jr. 1977. "Some Aspects of Wind Power Statistics." *J. Appl. Meteorol.,* 16 (2): 119–128. https://doi.org/10.1175/1520-0450(1977)016<0119:SAOWPS>2.0.CO;2.

Hirth, L., and S. Müller. 2016. "System-Friendly Wind Power- How Advanced Wind Turbine Design can Increase the Economic Value of Electricity Generated Through Wind Power." *Energy Economics,* 56 (May): 51–63. https://doi.org/10.1016/j.eneco.2016.02.016.

Johansson, V., and L. Thorson. 2016. "Modeling of Wind Power: A Techno-Economic Analysis of Wind Turbine Configurations." M.S. thesis. Dept. of Energy and Environment, Chalmers University of Technology.

Kelley, N., M. Shirazi, D. Jager, S. Wilde, E. G. Patton, and P. Sullivan. 2004. *Lamar Low-Level Jet Project Interim Report.* NREL/TP-500-34593. Golden, CO: National Renewable Energy Laboratory.

King, J., A. Clifton, and B. M. Hodge. 2014. *Validation of Power Output for the WIND Toolkit*. NREL/TP-5D00-61714. Golden, CO: National Renewable Energy Laboratory.

Lantz, E., O. Roberts, J. Nunemaker, E. DeMeo, K. Dykes, and G. Scott. 2019. *Increasing Wind Turbine Tower Heights: Opportunities and Challenges*. NREL/TP-5000-73629. Golden, CO: National Renewable Energy Laboratory.

List, R. J. 1951. *Smithsonian Miscellaneous Collections: Smithsonian Meteorological Tables.* vol. 114. 6th ed. Washington DC: Smithsonian Institution Press.

Meeker W. Q., and L. A. Escobar. 1998. *Statistical Methods for Reliability Data*. New York: Wiley.

MidAmerican Energy Company. 2015. MidAmerican Energy Installing First Concrete Wind Turbine Tower. Accessed September 10, 2020. https://www.brkenergy.com/news/midamerican-energy-installing-first-concrete-wind-turbine-tower

MISO (Midcontinent Independent System Operator). 2014. "Archived Historical Hourly Wind Data." Accessed April 8, 2018. https://www.misoenergy.org/markets-and-operations/real-time--market-data/market-reports/market-report-archives/#nt=%2FMarketReportType%3ASummary%2FMarketReportName%3AArchived%20Historical%20Hourly%20Wind%20Data%20%20(zip)&t=10&p=0&s=MarketReportPublished&sd=desc.

Moné, C., M. Hand, B. Maples, and A. Smith. 2015. *2013 Cost of Wind Energy Review*. NREL/TP-5000-63267. Golden, CO: National Renewable Energy Laboratory.

Petersen, E. L., N. G. Mortensen, L. Landberg, J. Højstrup, and H. P. Frank. 1998. "Wind Power Meteorology. Part I: Climate and Turbulence." *Wind Energy,* 1 (1): 2–22. https://doi.org/10.1002/(SICI)1099-1824(199809)1:1<2::AID-WE15>3.0.CO;2-Y.

Redburn, R. 2007. "A Tall Tower Wind Investigation of Northwest Missouri." M.S. thesis. Dept. of Soil, Environmental and Atmospheric Sciences, Univ, of Missouri.

Schwartz, M., and D. Elliott. 2005. "Towards a Wind Energy Climatology at Advanced Turbine Hub-Heights." NREL/CP-500-38109. In *Proc., 15th Conf. Appl. Climatol.*, 1–11. Savannah, GA: American Meteorological Society.

Showers, D. 2014. "System Identification for the Clipper Liberty C96 Wind Turbine." M.S. thesis, Dept. of Aerospace Engineering and Mechanics, Univ. of Minnesota.

Smith, K., G. Randall, D, Malcolm, N, Kelley, and B, Smith. 2002. "Evaluation of Wind Shear Patterns at Midwest Wind Energy Facilities." In *Proc. AWEA WINDPOWER*. Portland, OR: AWEA.

Sritharan, S. 2017. "Hexcrete Tower for Harvesting Wind Energy at Taller Hub Heights - Budget Period 2." Technical Rep. Washington, DC: Office of Energy Efficiency and Renewable Energy.

Storm, B., J. Dudhia, S. Basu, A. Swift, and I. Giammanco. 2009. "Evaluation of the Weather Research and Forecasting Model on Forecasting Low-Level Jets: Implications for Wind Energy." *Wind Energy*, 12 (1): 81–90. https://doi.org/10.1002/we.288.

Studylib. 2017. "The New Productivity Benchwork: Siemens Wind Turbine SWT-2.3-108." Siemens Market-Specific Solution. Accessed July 18, 2017. https://studylib.net/doc/10458843/the-new-productivity-benchmark-siemens-wind-turbine-swt-2...

Takle, E. S., J. M. Brown, and W. M. Davis. 1978. "Characteristics of Wind and Wind Energy in Iowa." *Iowa State J Res*, 3 (2): 313–339.

Walton, R. A., E. S. Takle, and W. A. Gallus. 2014. "Characteristics of 50-200-m Winds and Temperatures Derived from an Iowa Tall-Tower Network." *J Appl Meteorol Climatol*, 53 (10): 2387–93. https://doi.org/10.1175/JAMC-D-13-0340.1.

Wiser, R., M. Bolinger, G. Barbose, N. Darghouth, B. Hoen, A. Mills, et al. 2019. "2018 Wind Technologies Market Report." DOE/GO- 102019-5191. Washington, DC: DOE.

Wiser, R., D. Millstein, M. Bolinger, S. Jeong, and A. Mills. 2020. "The Hidden Value of Large-

Rotor, Tall-Tower Wind Turbines in the United States." *Wind Eng.*, 1-15. https://doi.org/10.1177/0309524X20933949.

Table 1. Summary of locations of meteorological towers

Location	Terrain Exposure	Meteorological Tower Instrumented Heights	Data Period and Data Variables
Homestead, Iowa (IA)	Hilly, rural area with a river to the north	Four heights: 50, 100, 150, and 200 m (Applies to Homestead, Altoona, Quimby, Mason City, and Palmer that did not have measurements at 200 m)	December 2006 – April 2009; data variables include wind speed and direction, and air temperature (Applies to Homestead, Altoona, Quimby, Mason City, and Palmer)
Altoona, IA	Suburban housing surrounding with a flat area to the southeast		
Quimby, IA	Hilly, rural area with a small river to the southeast		
Mason City, IA	Flat, rural area with a lake to the southeast, urban area to the southwest		
Palmer, IA	Flat, rural area with a lake to the northeast		
Rosemount, Minnesota (MN)	Flat, rural area with the Twin Cities urban area to the north	Ten heights: 125.9, 101.5, 76.7, 51.5, 27.1, 7.3, 127.9, 79.1, 29.6, and 9.9 m	One-month data in July 2014; data variables include wind speed and direction, air temperature, relative humidity, and barometric pressure at 76.7 m

Table 2. Summary of missing or unavailable wind data in Homestead

Height	Wind Speed		Wind Direction	
	Daytime	Nighttime	Daytime	Nighttime
50 m	1.33%	1.59%	13.33%	9.4%
100 m	3.65%	3.17%	37.75%	35.71%
150 m	4.46%	4.21%	13.68%	11.12%
200 m	30.85%	36.29%	40.71%	42.61%

Table 3. The AEP and capacity factor (CF) obtained by averaging the production from all five sites in Iowa

Height (m)	Average AEP 2.3 MW (MWh)	Average CF 2.3 MW (%)	Percent Change 2.3 MW	Average AEP 3.2 MW (MWh)	Average CF 3.2 MW (%)	Percent Change 3.2 MW
80	8.40×10^3	41.7		10.4×10^3	37.0	
100	9.18×10^3	45.5	9%*	11.5×10^3	40.9	10%*
120	9.45×10^3	46.9	13%*	11.9×10^3	42.6	15%*
140	9.82×10^3	48.7	17%*	12.5×10^3	44.6	20%*

*with respect to 80 m tower

Table 4. Comparison of annual energy production and net capacity factor for Homestead at 100 m

Parameters	NREL WIND Toolkit	Met-Tower Data	NREL WIND Toolkit	Met-Tower Data
Tower hub height, m	100	100	100	100
Turbine size, kW	2300	2300	3200	3200
Wind speed at 50 m height, m/s	6.51	6.72 (+3%)	6.51	6.72 (+3%)
Average power law α	0.248	0.248	0.248	0.248
Altitude at the hub height*, m	550	550	550	550
Air density at 80 m height, kg/m^3	1.163	1.163	1.163	1.163
Cut-in wind speed, m/s	3	3	3	3
Cut-out wind speed, m/s	25	25	25	25
Annual energy production, MWh/year	8,433	9,056 (+7.4%)	10,479	11,274 (+7.6%)
Net capacity factor (%)	41.9	44.9 (+7.4%)	37.4	40.2 (+7.6%)

*Altitude of ground surface assumed to be 450 m above sea level in the Midwest region

LIST OF FIGURES

Figure 1. Annual average wind speed in Iowa at 80 m height. The squares denote the site of a tall meteorological tower used for assessing wind power potential. (Map from DOE 2010, courtesy of DOE; map data © 2019 AWS Truepower and the National Renewable Energy Laboratory.)

Figure 2. Diurnal variation of measured wind speed at 100 m in Homestead

Figure 3. (a) Variations and (b) probability distribution of the 50-150-m power-law exponent at Homestead from measured data

Figure 4. (a) Diurnal and (b) seasonal cycles of the normalized energy production from measurements (MET) and MISO (MISO) compared to the average value of the energy production from measurements (MET_avg)

Figure 5. Diurnal variation of the power-law exponent from 50-150 m at multiple observed sites

Figure 6. Diurnal variations of the annual average of wind speed at various heights

Figure 7. (a) Capacity factors and (b) their percentage increases for a 2.3 MW turbine at hub heights in Iowa sites

Figure 8. (a) Capacity factors and (b) their percentage increases for a 3.2 MW turbine at hub heights in Iowa sites

Figure 9. Capacity factors for Rosemount in July and the average capacity factors for IA sites in summer (JJA) at different hub heights

Figure 10. (a) Variations of modeled wind speed with time, and (b) seasonal average of daytime (DT) and nighttime (NT) wind speeds from WIND Toolkit (WTK) and Observations (MET) in Homestead

Figure 11. Wind rose of wind speed in the season of (a) DJF, (b) MAM, (c) JJA, and (d) SON for Homestead from WIND Toolkit and measured data

Figure 12. Comparison of daytime (DT) and nighttime (NT) energy production in Homestead between measured (MET) and WIND Toolkit (WTK) data using measured and 1/7 power-law exponents for (a) 2.3MW and (b) 3.2 MW turbine

Figure 13. Comparison of capacity factor averaged for the IA sites between measured and WIND Toolkit data using measured and 1/7 power-law exponents

Iowa - Annual Average Wind Speed at 80 m

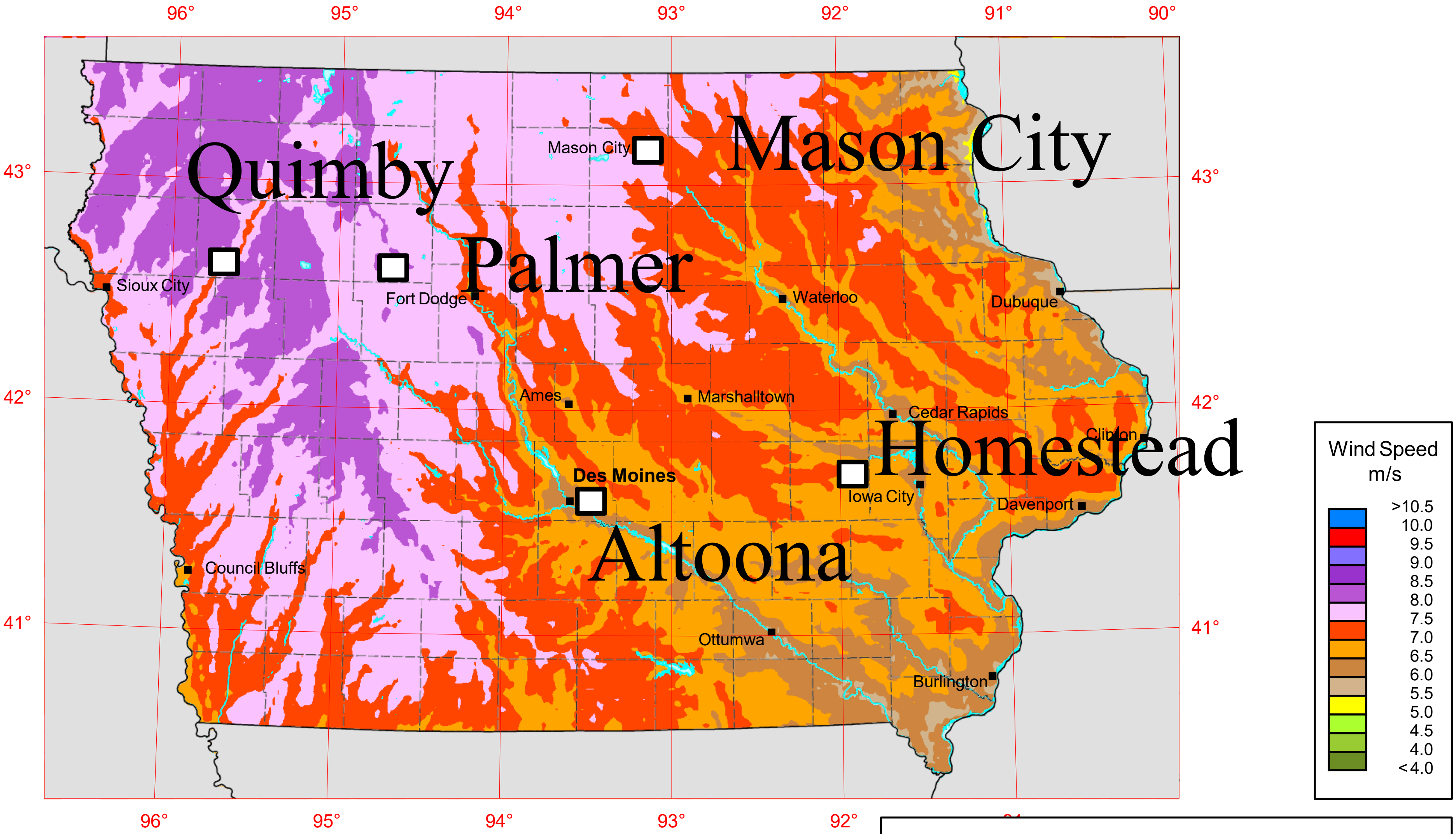
96°
95°
94°
93°
92°
91°
90°
43°
42°
41°
Quimby
Palmer
Mason City
Homestead
Altoona
Mason City
Sioux City
Fort Dodge
Waterloo
Dubuque
Ames
Marshalltown
Cedar Rapids
Clinton
Des Moines
Iowa City
Davenport
Council Bluffs
Ottumwa
Burlington
Wind Speed
m/s
>10.5
10.0
9.5
9.0
8.5
8.0
7.5
7.0
6.5
6.0
5.5
5.0
4.5
4.0
< 4.0

Source: Wind resource estimates developed by AWS Truepower, LLC for windNavigator®. Web: http://www.windnavigator.com | http://www.awstruepower.com. Spatial resolution of wind resource data: 2.5 km. Projection: UTM Zone 15 WGS84.

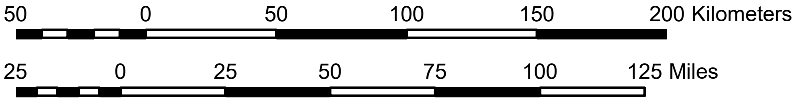
50
0
50
100
150
200 Kilometers
25
0
25
50
75
100
125 Miles

AWS Truepower™
Where science delivers performance.

NREL
NATIONAL RENEWABLE ENERGY LABORATORY

11-OCT-2010 1.1.1

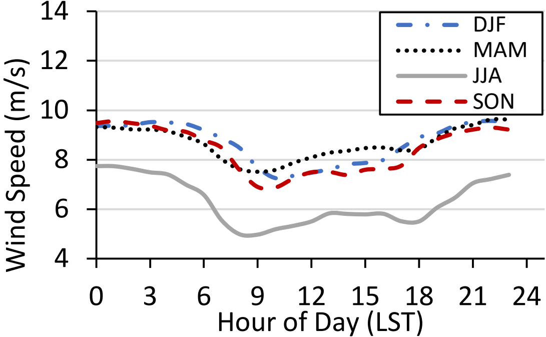
Wind Speed (m/s)
14
12
10
8
6
4
0
3
6
9
12
15
18
21
24
Hour of Day (LST)
DJF
MAM
JJA
SON

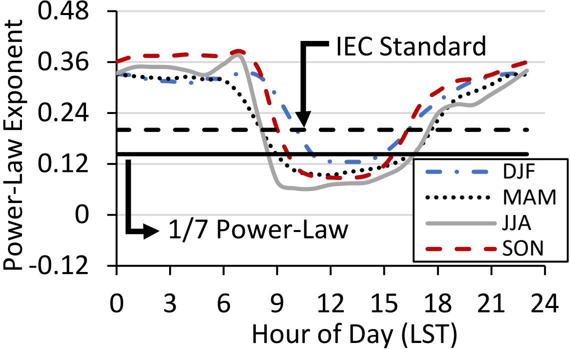
0.48
0.36
0.24
0.12
0
-0.12
Power-Law Exponent
IEC Standard
1/7 Power-Law
DJF
MAM
JJA
SON
0
3
6
9
12
15
18
21
24
Hour of Day (LST)

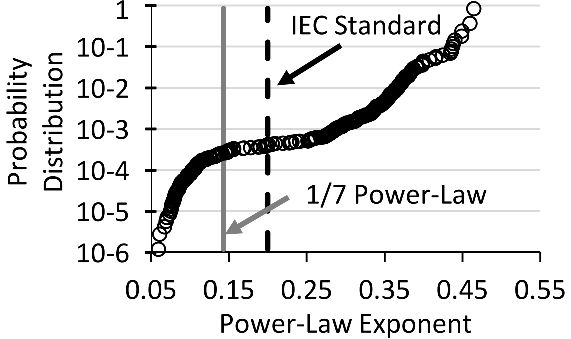

IEC Standard
1/7 Power-Law
Probability Distribution
1
10-1
10-2
10-3
10-4
10-5
10-6
0.05
0.15
0.25
0.35
0.45
0.55
Power-Law Exponent

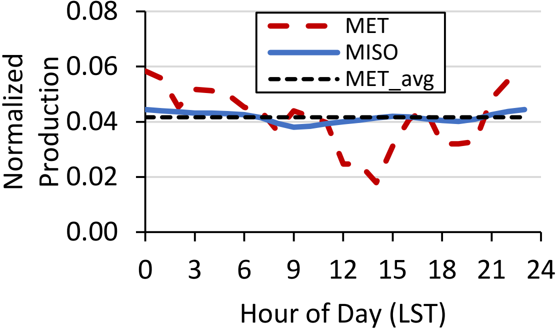
Normalized Production
0.08
0.06
0.04
0.02
0.00
0
3
6
9
12
15
18
21
24
Hour of Day (LST)
MET
MISO
MET_avg

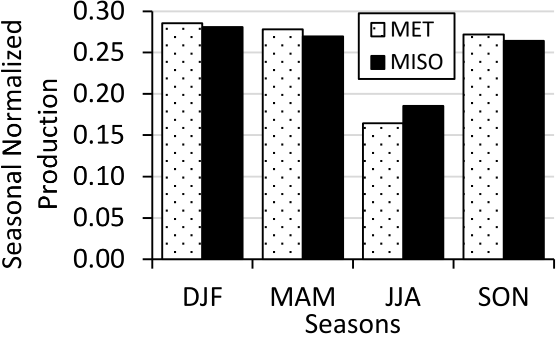

Seasonal Normalized Production
0.30
0.25
0.20
0.15
0.10
0.05
0.00
MET
MISO
DJF
MAM
JJA
SON
Seasons

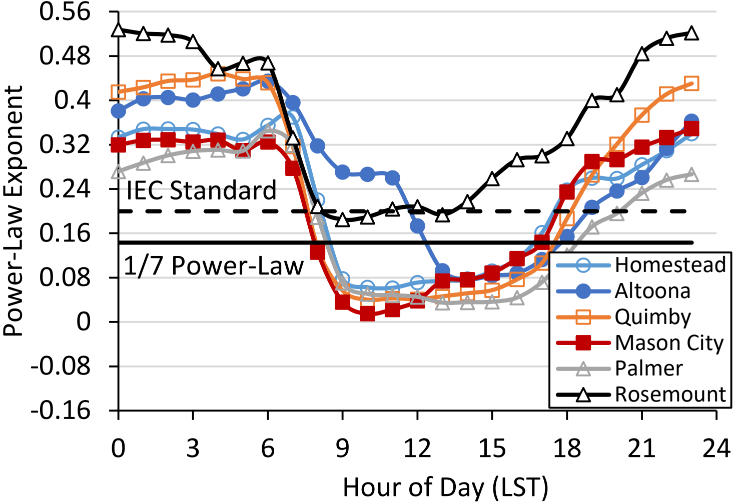
0.56
0.48
0.4
0.32
0.24
0.16
0.08
0
-0.08
-0.16
Power-Law Exponent
IEC Standard
1/7 Power-Law
0
3
6
9
12
15
18
21
24
Hour of Day (LST)
Homestead
Altoona
Quimby
Mason City
Palmer
Rosemount

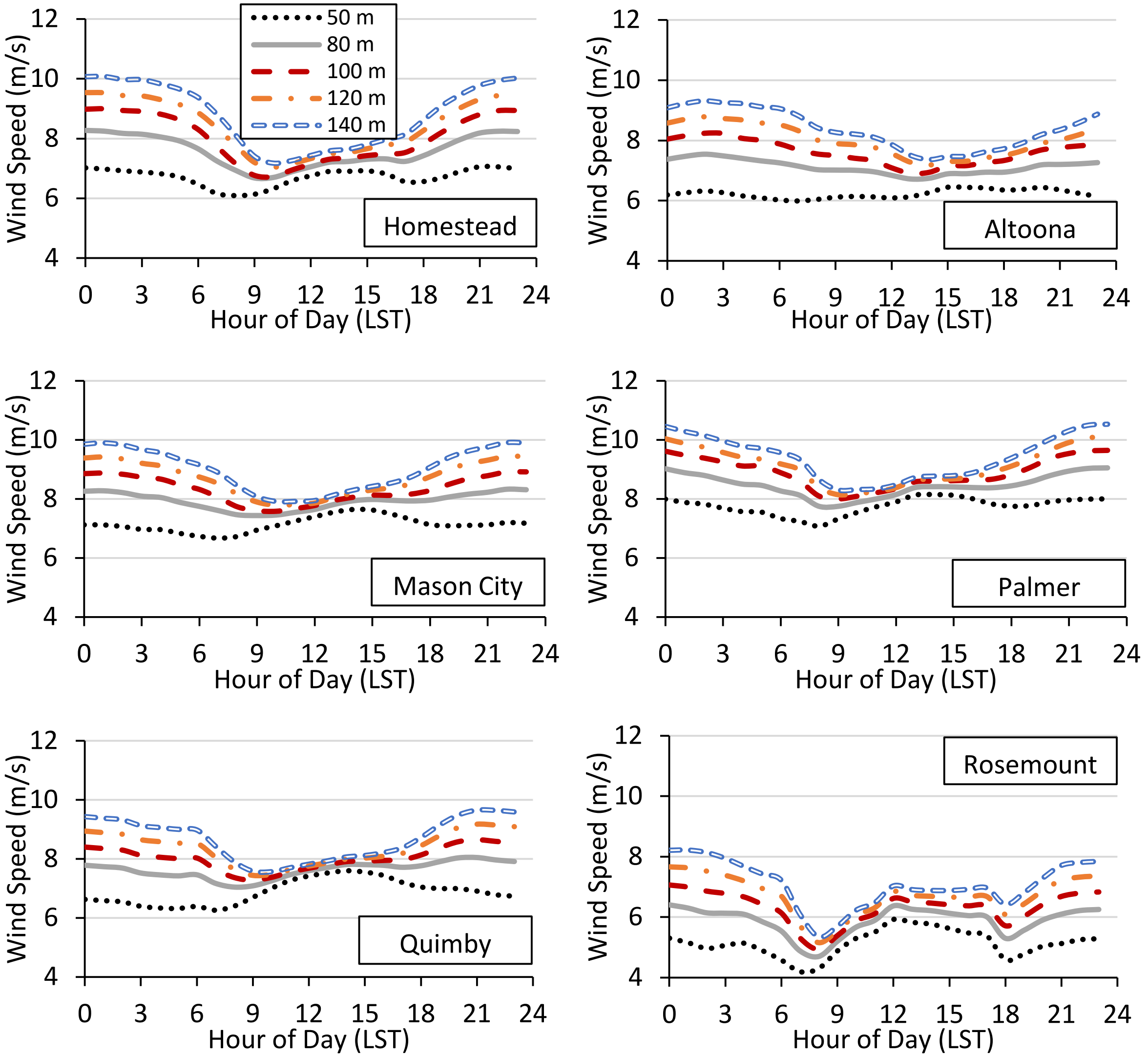
50 m
80 m
100 m
120 m
140 m
Homestead
Altoona
Mason City
Palmer
Quimby
Rosemount
Wind Speed (m/s)
Hour of Day (LST)
4
6
8
10
12
0
3
6
9
12
15
18
21
24

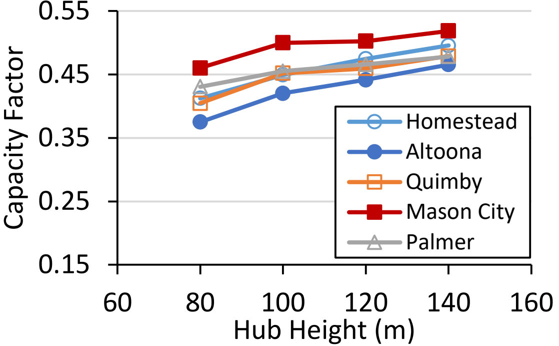
0.55
0.45
0.35
0.25
0.15
Capacity Factor
60
80
100
120
140
160
Hub Height (m)
Homestead
Altoona
Quimby
Mason City
Palmer

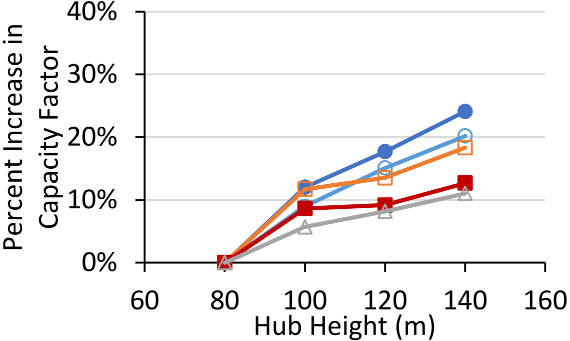
40%
30%
20%
10%
0%
Percent Increase in Capacity Factor
60
80
100
120
140
160
Hub Height (m)

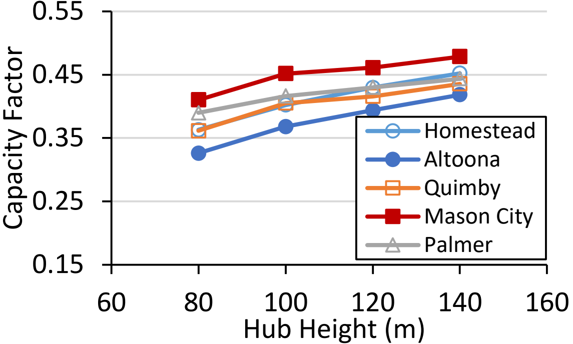
Capacity Factor
0.55
0.45
0.35
0.25
0.15
60
80
100
120
140
160
Hub Height (m)
Homestead
Altoona
Quimby
Mason City
Palmer

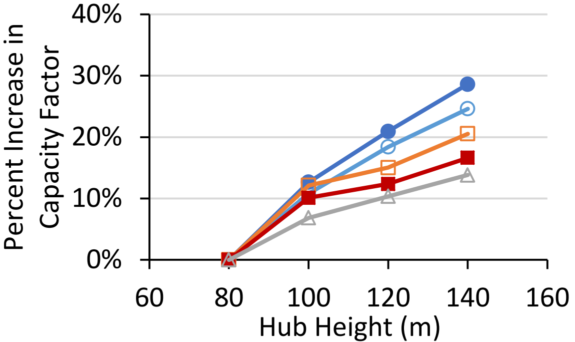
Percent Increase in Capacity Factor
40%
30%
20%
10%
0%
60
80
100
120
140
160
Hub Height (m)

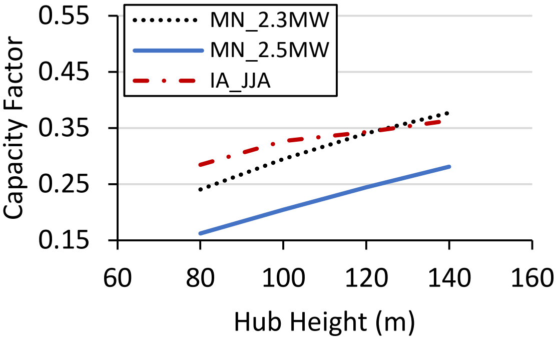
MN_2.3MW
MN_2.5MW
IA_JJA
Capacity Factor
0.55
0.45
0.35
0.25
0.15
60
80
100
120
140
160
Hub Height (m)

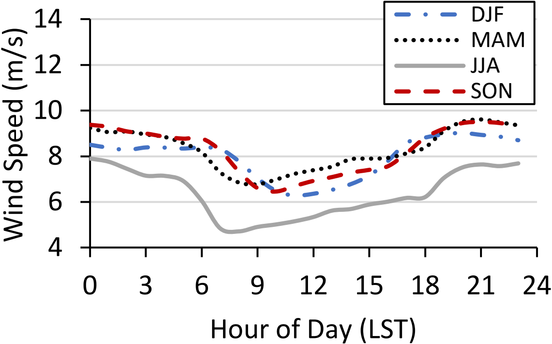
DJF
MAM
JJA
SON
Wind Speed (m/s)
4
6
8
10
12
14
0
3
6
9
12
15
18
21
24
Hour of Day (LST)

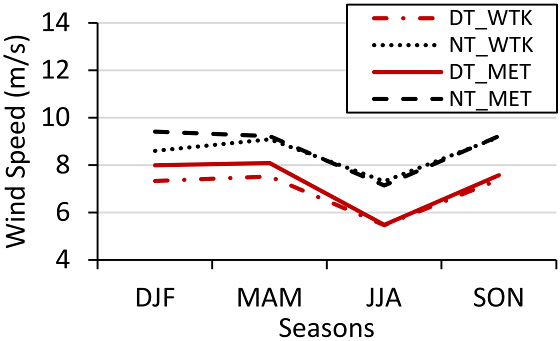
DT_WTK
NT_WTK
DT_MET
NT_MET
Wind Speed (m/s)
14
12
10
8
6
4
DJF
MAM
JJA
SON
Seasons

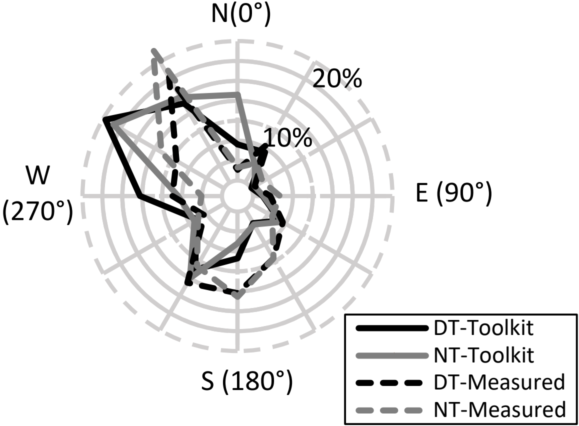
N(0°)
20%
10%
E (90°)
W
(270°)
S (180°)
DT-Toolkit
NT-Toolkit
DT-Measured
NT-Measured

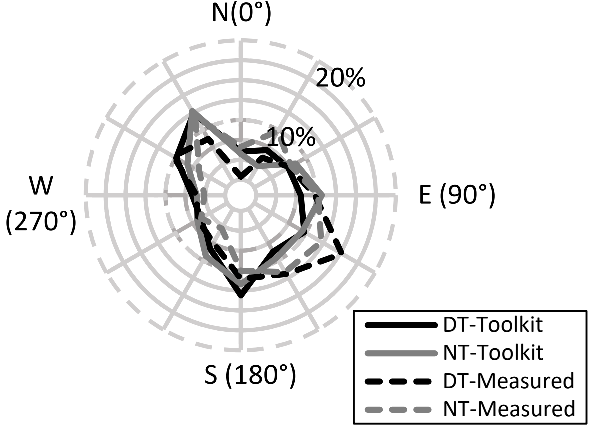
N(0°)
20%
10%
E (90°)
W
(270°)
S (180°)
DT-Toolkit
NT-Toolkit
DT-Measured
NT-Measured

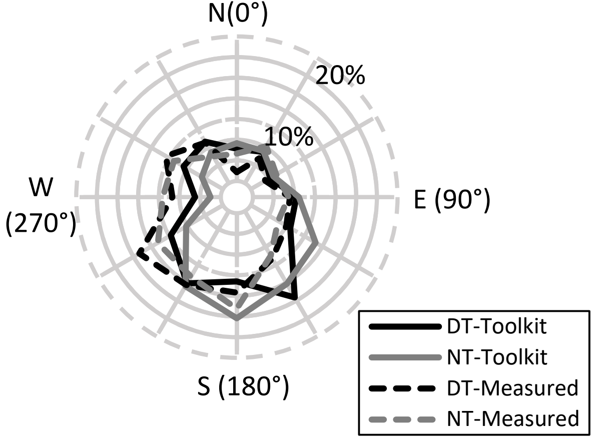
N(0°)
20%
10%
E (90°)
W
(270°)
S (180°)
DT-Toolkit
NT-Toolkit
DT-Measured
NT-Measured

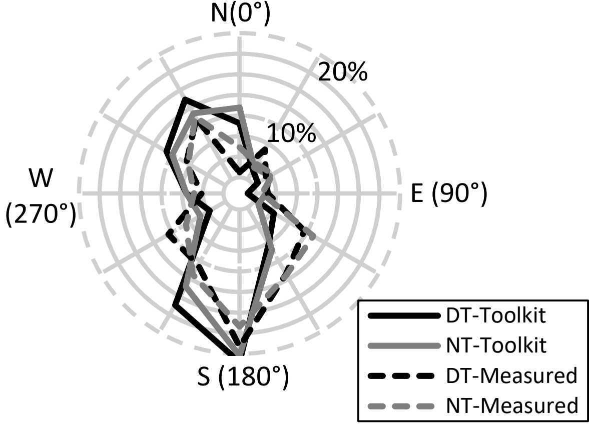
N(0°)
20%
10%
W
(270°)
E (90°)
S (180°)
DT-Toolkit
NT-Toolkit
DT-Measured
NT-Measured

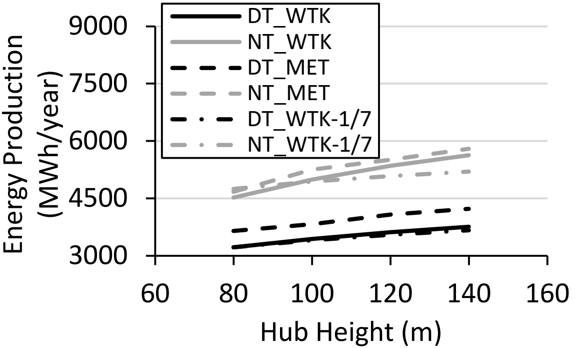
DT_WTK
NT_WTK
DT_MET
NT_MET
DT_WTK-1/7
NT_WTK-1/7
Energy Production (MWh/year)
9000
7500
6000
4500
3000
60
80
100
120
140
160
Hub Height (m)

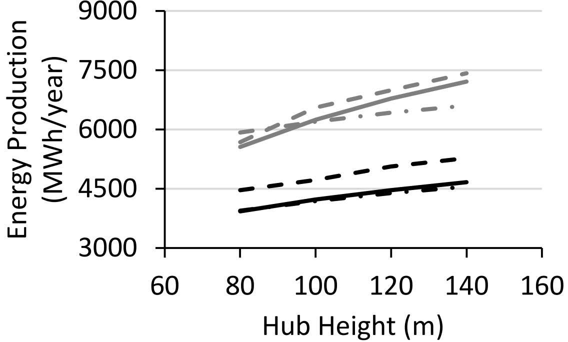
9000
7500
6000
4500
3000
Energy Production (MWh/year)
60
80
100
120
140
160
Hub Height (m)

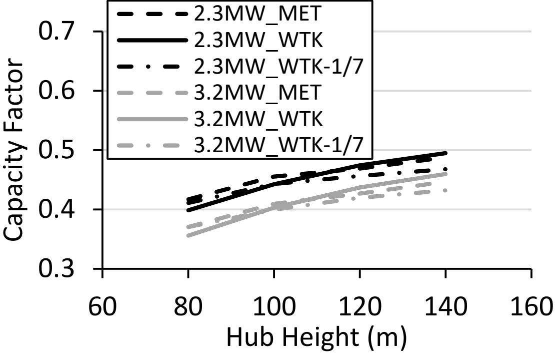
2.3MW_MET
2.3MW_WTK
2.3MW_WTK-1/7
3.2MW_MET
3.2MW_WTK
3.2MW_WTK-1/7
Capacity Factor
0.7
0.6
0.5
0.4
0.3
60
80
100
120
140
160
Hub Height (m)